Proceedings of the 2018 IEEE
International Conference on Robotics and Biomimetics
December 12-15, 2018, Kuala Lumpur, Malaysia

External Force Estimation of Impedance-Type Driven Mechanism for Surgical Robot with Kalman Filter

Hongbing Li, Kundong Wang, Zheng Li, Kenji Kawashima, and Evgeni Magid

***Abstract*—Haptic feedback has been proved the importance in the surgical robot system, however, such function is missing in current commercially available minimally invasive surgical robot system. To address this issue, many surgical forceps have been designed and developed to provide the sense of contact forces to the surgeon during surgical manipulation. However, to data, there are no commercially available surgical forceps with haptic perception because of the disadvantages of such physical-sensing devices. No matter what sensing algorithm it utilized, there are always physical constraints related to the force sensors. This study presents concepts and application of a Kalman filter for the control of robot handle force during contact with the external environment. The external contact force in the system was estimated by parameter estimation techniques to the robot actuators. The method is described and its effectiveness is shown for a one degree-of-freedom robot.**

***Index Terms*—Sensorless external force estimation, Kalman filter, robot surgery.**

I. Introduction

HAPTIC perception plays a very important role in surgery. It enables surgeons to obtain the mechanical properties of tissue and evaluate its anatomical structures. Most importantly, it applies appropriate force control actions for safe tissue manipulations. The necessity of force feedback has motivated intensive research on the design of surgical instruments with force perception capabilities. In general, two main approaches to enable force-sensing ability are commonly seen in surgical applications. The most common method used to solve the problems due to the lack of force sensing ability is the utilization of mechanical or electrical sensors, which are integrated with surgical instruments, such as displacement sensors proposed by Rosen [1], strain gauge sensors proposed by Trejos [2], Okamura [3], Hong [4], Baki [5], and Hu [6], capacitive sensors proposed by Lee [7], [8], and Kim [9], [10], piezoelectric-based sensors proposed by Qasaimeh [11], optical fiber sensors proposed by Peris [12], Puangmali [13], and Haslinger [14], and miniaturized vibro-tactile sensors proposed by Omata [15], Ohtsuka [16], Fetter [17]. However, due to the size, cost, and environmental requirements of minimally invasive surgery (MIS), few commercially available force sensors can be directly used in surgery. A complete review of the force and tactile sensing technologies applied in MIS can be found in [18].

An alternative way to develop a force sensing surgical device is the sensorless approach. In the absence of force sensors, interaction force information can be obtained by estimation, utilizing other sources of available or measurable information such as the position/velocity of the robot, torque applied by the robot's actuators, and the robot's physical parameters. Although contacting force estimation methods have good performance in the field of MIS, few researches were conducted on this method in the context of force control of surgical robot. Ohishi et al. [19] proposed an acceleration controller with hybrid force and position control for robot system. They used a disturbance observer to estimate contact forces. Recently, Li et al. [20] developed four degree-of-freedom (DOF) pneumatic driven forceps that has the force perception capabilities. In this system, the delicate force sensing is achieved by using a disturbance observer to the pneumatic driving system. Zhao and Nelson [21]-[23] explore the feasibility of driving motor currents for the sensorless estimation of tool-tissue interaction forces for a decoupled 3-DOF surgical grasper. However, the dynamic effect of the grasper is neglected and the friction in the transmission mechanism is also ignored. Li et al. [24] and Haghighipanah et al. [25] estimated the external contact force of the cable driven surgical robot utilizing system dynamics and the square root unscented Kalman filter. However, it was determined that the friction in the transmission and cable properties greatly affect the accuracy of the dynamic model. To solve this problem, Li

This work was partially supported by Project of International Academic Cooperation and Exchanges of Shanghai under Grant 16550720100, and by Natural Science Foundation of Shanghai under Grant 18ZR1421300, and by the National Natural Science Foundation of China under Grant 51505280, and by Projects of Science and Technology Commission Shanghai Municipality under Grant 18511108202.

Hongbing Li is with the Department of Instrument Science and Engineering, Shanghai Jiaotong University, Shanghai, China (corresponding author to provide phone: 86-21-3420-5206; fax: 86-21-3420-5372; e-mail: lihongbing@sjtu.edu.cn).

Kundong Wang is with the Department of Instrument Science and Engineering, Shanghai Jiaotong University, Shanghai, China (e-mail: kdwang@sjtu.edu.cn).

Zheng Li is with the Department of Surgery, The Chinese University of Hong Kong, Shatin, Hong Kong (e-mail: lizheng@cuhk.edu.hk).

Kenji Kawashima is with Department of Biomechanics, Tokyo Medical and Dental University, Tokyo, Japan.(e-mail: kkawa.bmc@tmd.ac.jp).

Evgeni Magid is with the Higher Institute of Information Technology and Information Systems, Kazan Federal University, Kazan, Russia (e-mail: dr.e.magid@ieee.org).

978-1-7281-0377-8/18/$31.00 © 2018 IEEE

and Hannaford [26] proposed four Gaussian process regression filters to address model uncertainties and nonlinearity for gripping force estimation of elongated cable-driven surgical instruments without using force sensor. However, the proposed estimator must be trained with hundreds of data points, which require great system computation time. Most recently, Sang et al. [27] estimated the external force based on the dynamic model of the open-loop surgical manipulator and driving motor current. The dynamic model of the patient side robot was derived using screw theory, Lagrange dynamics and rotor dynamics of the servo motors. Nevertheless, the proposed external force estimation method is sensitive to the model parameters.

In above aforementioned applications that use torque observers to estimate the grasping force of the robotic forceps, a linear DC motor is commonly used as an actuator. The DC motor is with the features of low inertia moment, no cogging, low friction, and very compact commutation. As a result, these good features in turn results in high acceleration, high efficiency, low joule losses and higher continuous output torque. Commonly, the surgical robot system is a small-scale design and does not require high joint speeds. Therefore, the most commonly adopted actuation unit structure is to use the combination of a small, low-power motor with high gear reduction, such as the snake-like surgical robot [28], Raven-II surgical robot [25], [26], S-Surge surgical robot [10], 3-DOF motorized surgical grasper [21]-[23], and da Vinci surgical robot [29]. In general, surgical forceps with highly geared drive mechanisms are either non-backdrivable or difficult to backdrive. It is clearly impossible to use motor current to measure external applied force in a stationary non-backdrivable system because the external contact force is not transmitted to the driving motor. The driving torque of the DC motor includes not only the useful external contact force, but also the noise torque, which is a combination of the load torques caused by the reduction gear and the component parts of the robot. As a result, the external contact force cannot be accurately estimated through the current of the DC motor.

In this study, the Kalman filter method is applied it on a backdrivable mechanism that can be used as the driven unit for surgical robot system. The external contact force on the end joint of the forceps is estimated by the current of the DC motor. As the current signal of the motor is noisy and a specially designed current sensor is also needed for the current measurement, a Kalman filter is used to predict the driving current of the DC motor. The estimated contact force of the end joint is compared with the actual measured one from the force sensor.

This remainder of this paper is organized as follows. In section II, the model of the DC motor and Kalman filter is introduced. In section III, the system dynamics and external force estimation algorithm is presented. Section IV describes the experimental setup and system parameters. Section V provides results with discussion. Finally, section VI discusses the results and concludes the paper.

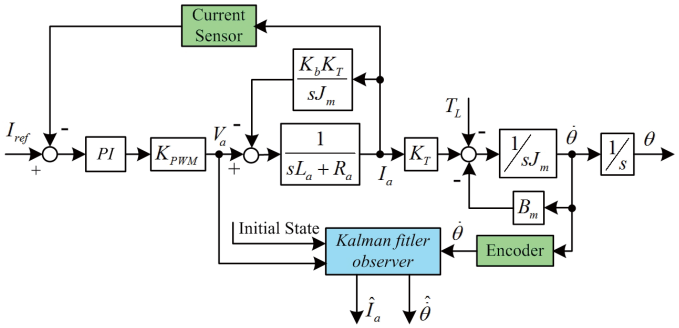

Fig.1. Model of the linear DC motor regulated under the ideal current source with a Kalman filter.

II. Estimation Methods

Given the torque in the driving DC motor of the surgical forceps is proportional to the current in the motor servo amplifier. This can be used to apply external force estimation. Ideally, the current of the motor should be found without adding any other sensors. Instead, it is very useful if an already installed transducer, such as the position sensor, could be utilized. Figure 1 presents the model of the DC motor regulated under the current source with Kalman filter. A PI current controller is utilized in the amplifier of the DC motor using the sensing current signal of the driver. A high resolution optical encoder is used to measure the position of the end joint. Also this position signal acts as the input signal to the Kalman filter with the driving voltage of the robot handle for estimating the driving current and velocity.

A. Armature Controlled DC Motor

An armature-controlled DC motor is employed in this study to perform state prediction. The transfer function of a DC motor is derived as

$$\frac{\theta(s)}{V_a(s)} = \frac{K_t}{s\left[(sL_a + R_a)(sJ_m + B_m) + K_t K_b\right]} \tag{1}$$

where θ is the position of the motor shaft, V_a is the applied voltage, L_a is the armature winding inductance, R_a is the armature winding resistance, J_m is the moment of inertia of rotor and load, B_m is the damping coefficient, K_t is the motor torque constant, and K_b is the back emf constant.

Define $\dot{\theta}$ and i_a as the state variables, so that the state vector is $X = \left[i_a, \dot{\theta}\right]^T$, where $\dot{\theta} = d\theta/dt$. In measurement, the rotating speed of the driving motor shaft is the output. Accordingly, the continuous state equations of the DC motor are

$$\frac{d}{dt}\begin{bmatrix} i_a \\ \dot{\theta} \end{bmatrix} = \begin{bmatrix} -R_a/L_m & -K_b/L_m \\ K_t/J_m & -B_m/J_m \end{bmatrix}\begin{bmatrix} i_a \\ \dot{\theta} \end{bmatrix} + \begin{bmatrix} 1/L_m \\ 0 \end{bmatrix} u \tag{2}$$

$$y = \begin{bmatrix} 0 & 1 \end{bmatrix}\begin{bmatrix} i_a \\ \dot{\theta} \end{bmatrix} \tag{3}$$

The general form of the state equations for a continuous system are

$$\dot{V}(t) = A_c V(t) + B_c U(t),\ Y(t) = C_c V(t) + D_c U(t) \tag{4}$$

where $V(t)$ is the variation of the estimated rotating speed. A_c, B_c C_c, and D_c are the coefficient matrices of the state equation for a continuous system. Let $\Phi_c(t) = L^{-1}\left[(sI - A_c)^{-1}\right]$ be the state transition matrix for (4), where $L^{-1}[\bullet]$ denotes the inverse Laplace transform. The discrete state equations sampled from the above equations by a sample-and-hold with time interval T seconds are as follows:

$$X_{k+1} = A_d X_k + B_d U_k \tag{5}$$

$$Y_k = C_d X_k + D_d U_k \tag{6}$$

where A_d, B_d, C_d, and D_d are the coefficient matrices of the state equation for the discrete system, which are calculated by the following equations:

$$A_d = \Phi_c(t),\ B_d = \left[\int_0^T \Phi_c(\tau)d\tau\right]B_c,\ C_d = C_c,\ D_d = D_c$$

B. Kalman Filter for State Estimation

A Kalman filter is a commonly used linear optimal observer, which estimates the system state, given a system model, input, and measurement. In the least squares sense, Kalman filter minimizes the inconsistencies with all information available to obtain the best possible estimation. State estimates and measurements are expressed as Gaussian distributions, express a desired level of confidence on the information. The system model is composed of a state equation, measurement equation, measurement covariance matrices R, process covariance matrices Q, and initial state estimate $\hat{x}_0$ (with corresponding initial covariance matrix P_0). The differentiable state transition and observation models used in an extended Kalman filter are represented as follows:

$$\begin{cases} x_{k+1} = A_k x_k + B_k u_k + w_k \\ y_k = h(x_k) + v_k \end{cases} \tag{7}$$

where x_k is the state vector at time k, A_k is the state at the current step k, u is the control input, and y_k is the observation at time k with measurement prediction function $h(\bullet)$. Both the process noise w and observation noise v have Gaussian distributions.

It is assumed that the covariance matrix of the process noise Q, covariance matrices of the measurement noise R, and cross-covariance matrix are

$$Q = E\{\omega\omega^T\} > 0 \tag{8}$$

$$R = E\{vv^T\} \geq 0 \tag{9}$$

$$E\{\omega v^T\} = 0 \tag{10}$$

The bandwidth of the Kalman filter and its susceptibility to measurement noise all depend on its process noise covariance matrix Q and the measurement noise covariance matrix R. We will use these values to tune the accuracy and response of the observer. The matrices Q and R can be determined by using the simulations for the measurement sensors testing.

The measurement and state equations are linearized about the most recent state estimate in the Kalman filter. The two main steps constitute the filtering are: prediction and update. For prediction the state transition matrix A_{k-1} is computed as the Jacobian of the state function evaluated at the previous state estimate. In the update stage, the observation matrix H_k is computed as the Jacobian of the function $h(\bullet)$ with respect to the state vector x_k, where $(\dot{\bullet})$ and $(\hat{\bullet})$ are the prediction and estimates. The subscript $k|k-1$ is the computations at time k, given others at time $k-1$ and similarly for $k-1|k-1$ and $k|k-1$. The robust filtering algorithm based on the gain adjustment is unified in the following method.

1) State Prediction

The one-step state prediction and the covariance matrix are

$$\hat{x}_{k|k-1} = A_k \hat{x}_{k-1|k-1} + B_k u_k \tag{11}$$

$$P_{k|k-1} = A_{k-1} P_{k-1|k-1} {A_{k-1}}^T + W_{k-1} \tag{12}$$

2) Gain Adjustment

The covariance matrix of the prediction error is modified by

$$\sum_{k|k-1} = S\left(P_{k|k-1}\right) \tag{13}$$

where S is a gain scheduling operator.

3) Measurement Innovation

The innovation from measurements and its covariance matrix are

$$\hat{Y}_k = Y_k - H_{k-1}\hat{X}_{k|k-1} \tag{14}$$

$$\tilde{P}_k = H_{k-1}\sum_{k|k-1} {H^T}_{k-1} + V_k \tag{15}$$

4) Estimation Update

The filtering gain and estimation of state using the covariance matrix are

$$K_k = \sum_{k|k-1} {H^T}_k \tilde{P}^{-1} \tag{16}$$

$$\hat{X}_{k|k} = \hat{X}_{k|k-1} + K_k \hat{Y}_k \tag{17}$$

$$P_{k|k} = \left(\sum_{k|k-1}{}^{-1} + {H_k}^T {V_k}^{-1} H_k\right)^{-1} \tag{18}$$

III. System Dynamics

The robot torque and force is estimated by modeling the robot dynamics. The well-known robot dynamics and relationship between the force and torque on the end effector and joint torque on the robot is described by the following equations:

$$\tau_{ext} = J^T F \tag{19}$$

$$\tau_m = D(\theta)\ddot{\theta} + H\left(\theta,\dot{\theta}\right)\dot{\theta} + C(\theta) + \tau_f\left(\dot{\theta}\right) + \tau_{ext} \tag{20}$$

where τ_m is the vector of the torques of the DC motor exerted in each robot joint, J is the robot Jacobian, F is the vector of force ejected in the robot end effector, $J_m(\theta)$ is the robot inertia matrix, $H\left(\theta,\dot{\theta}\right)$ is the Coriolis forces vector, $C(\theta)$ is the gravity force vector, $\tau_f\left(\dot{\theta}\right)$ is the friction torque vector, and τ_{ext} is the external torques on each joint produced by external force on the end effector. By combining the above two equations, the external force at the tip is

$$F = \left(J^T\right)^{-1}\left(\tau_m - D(\theta)\ddot{\theta} - H\left(\theta,\dot{\theta}\right)\dot{\theta} - C(\theta) - \tau_f\left(\dot{\theta}\right)\right) \tag{21}$$

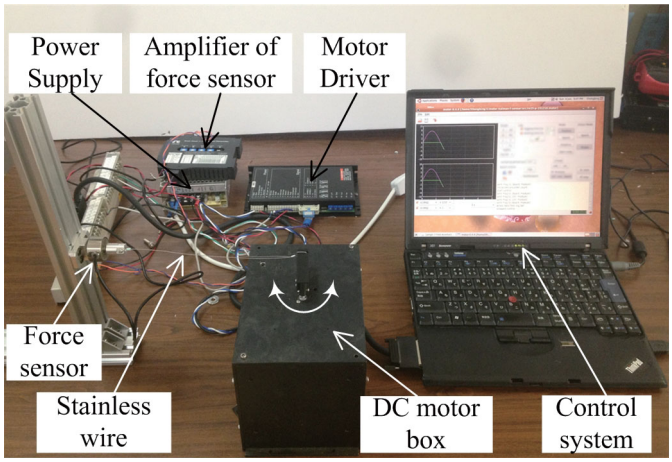

Fig.2. Experimental setup for sensorless force estimation.

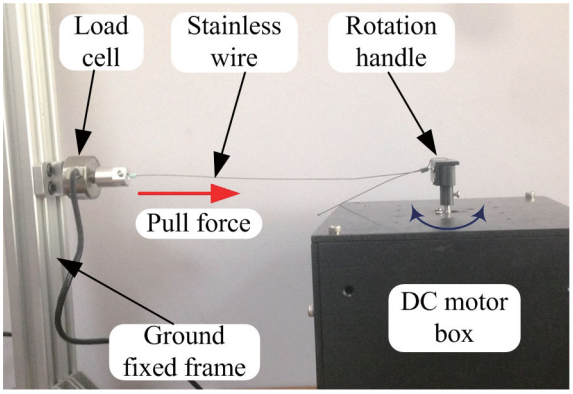

Fig.3. External contact force measurement setup.

We hypothesize that the external force on the robot tip for a backdrivable robot can be estimated by the driving current in the motor driver. Based on the current amplitude of each actuator and mathematical model it is possible to determine the external force excreted on a robot with backdrivability as.

$$\tau_m = K_t I_a \tag{22}$$

where K_t is the motor torque constant, and I_a is the current amplitude.

IV. Experimental Setup

The experimental setup, shown in Fig.2 is composed of a DC motor box with a driver unit, force sensor with an amplifier and data acquisition system.

A. The Driving DC Motor

The DC motor used in this experiment was made by Maxon, Switzerland which was driven by a PWM Amplifier (Maxon ADS 50-5). The model number of the motor is RE 25. Parameters for the DC motor used in this study are as follows: $V_a = 24V$, $B_m = 2.0\times10^{-6} Nms$, $L_a = 8.3\times10^{-4} H$, $R_a = 7.31\Omega$, $J_m = 1.05\times10^{-6} kgm^2$, $K_t = 0.044 Nm/\mathrm{A}$, and $K_b = 22.7 rad/Vs$. Substituting into (2) and (3), the continuous state equations of the motor become:

$$\frac{d}{dt}\begin{bmatrix} i_a \\ \dot{\theta} \end{bmatrix} = \begin{bmatrix} -8.78\times10^3 & -52.8 \\ 4.2\times10^4 & -1.9 \end{bmatrix}\begin{bmatrix} i_a \\ \dot{\theta} \end{bmatrix} + \begin{bmatrix} 1201.9 \\ 0 \end{bmatrix} u \tag{23}$$

$$y = \begin{bmatrix} 0 & 1 \end{bmatrix}\begin{bmatrix} i_a \\ \dot{\theta} \end{bmatrix} \tag{24}$$

The discrete state equations sampled from the above equations with time interval $T = 0.001s$ are

$$\begin{bmatrix} i_{a,k+1} \\ \dot{\theta}_{k+1} \end{bmatrix} = \begin{bmatrix} 0.12 & -0.0053 \\ 4.2 & 0.997 \end{bmatrix}\begin{bmatrix} i_{a,k} \\ \dot{\theta}_k \end{bmatrix} + \begin{bmatrix} 0.274 \\ 5.312 \end{bmatrix} u_k \tag{25}$$

$$y_k = \begin{bmatrix} 0 & 1 \end{bmatrix}\begin{bmatrix} i_{a,k} \\ \dot{\theta}_k \end{bmatrix} \tag{26}$$

B. Data Acquisition System

In order to maintain an accurate sampling, a real time control system based on Linux OS was installed and used. The controller of the one DOF system is implemented at the PC. The target PC contained an AD/DA multi-function card (CSI-360116, Interface Co., Ltd) for CardBus systems with differential A/D lines for reading the load cell, and D/A for outputting command signals to the motor amplifier. This card was also be used to read output pulse of the encoder signals from the optical encoder rotation sensor. The core controlling program ran for the duration of a block of trials, reading sensors and commanding motor torque at a rate of 1 kHz through experimental conditions.

An optical encoder (MEH-12-1000P, Microtech Laboratory Inc.) is used at the end axis of the DC motor to measure the rotational position of the handle. Velocity is not directly measured, it is obtained by differentiating the rotary position with respect to time. The external contact force is measured by a load cell (ZNLBM-1KG, Zhongnuo Co., Ltd) with a transmitter (DMD4059, Omega Co. Ltd).

V. Results and Discussion

The results are presented as graphs of the behavior to reference the input described in the previous section. In this section, we analytically compare the kinesthetic performance of the proposed current based external force estimation method. The proposed controller is experimentally evaluated in the following section.

A. Test-Position Tracking during Free Motion

First, it is assumed that the robot handle does not contact the external environment. The robot handle was driven by the sinusoid reference position signal with an amplitude of 6 deg at a frequency of 0.4Hz, and the experimental results are shown in Fig. 4. The position tracking performance of the robot handle is shown by Fig.4 (a). The robot handle can track the sinusoid reference position signal very well. The estimated velocity by the Kalman filter is shown in Fig.4 (b). The actual handle velocity calculated from the position signal of the optical encoder is close to the estimated one. Experimental results verified the effectiveness of the proposed control scheme. Fig.4 (c) shows the actual current of the motor measured by the current sensor installed at the motor amplifier. Compared with the noisy measured current signal, the estimated current from the Kalman filter has the advantage the noise rejection. As the robot handle does not contact the external environment, the measured force from the load cell is close to zero but noisy, as shown in Fig.4 (d).

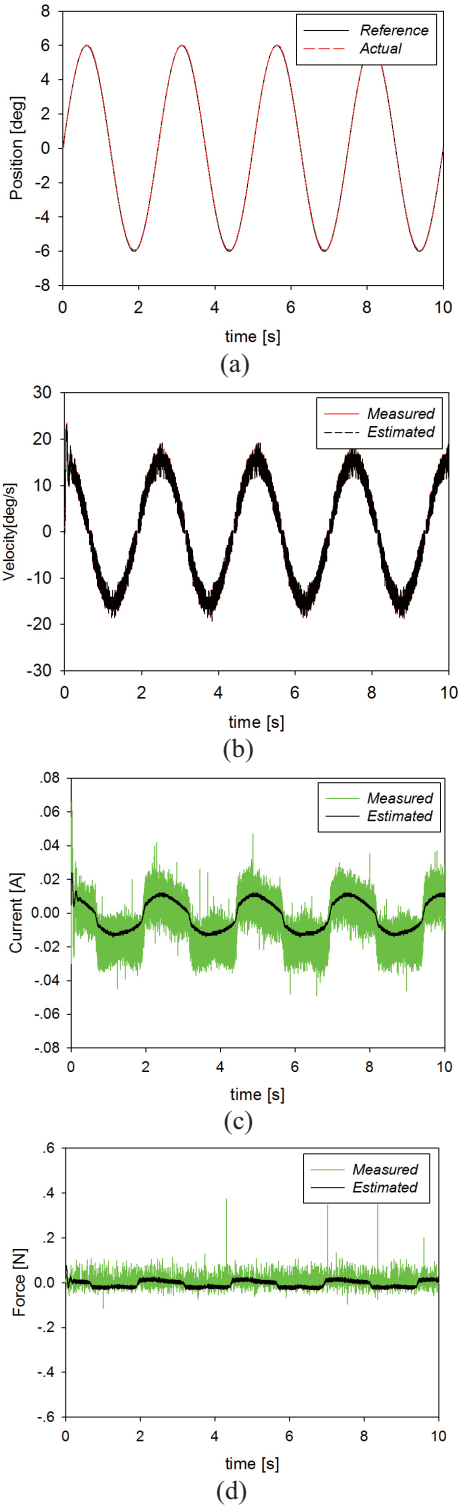

Fig.4. Free motion with Kalman filter estimation.

B. Test Position Tracking during Constrained Motion

For comparative analysis, the robot handle was connected to the load cell by a stainless steel wire with a diameter of 0.4mm (AB018-50FT, 7x7 strands, Berg Inc.), as shown in Fig.3. The load cell is fixed on a frame based on the ground. The estimated force at the handle tip is estimated by the calculated current from the Kalman filter. As a result, we can compare the accuracy of the external force estimation by the output of the load cell.

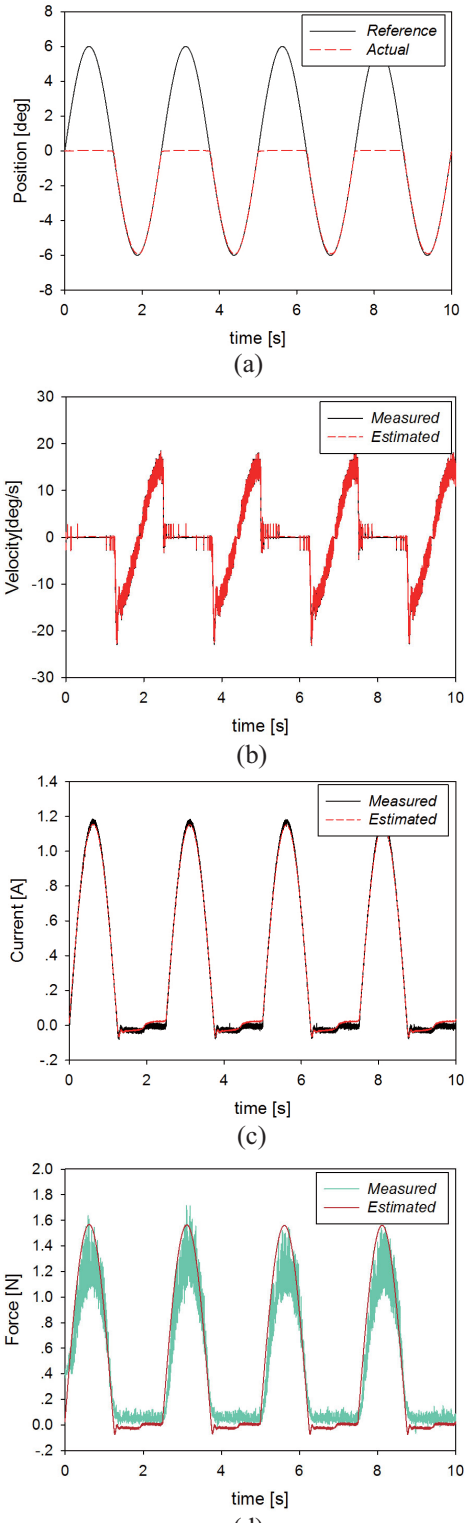

Fig.5. External force estimation by Kalman fitler.

Similar to the above free motion, the robot handle was also driven by the sinusoid reference position signal with a amplitude of 6 deg at a frequency of 0.4Hz. The experimental results are shown in Fig. 5. The robot handle is constrained by the stainless wire at the half of the reference trajectory as shown by Fig.5 (a). On the other half of the trajectory, the handle follows the reference trajectory very well. During this period,

the robot handle pulls the stainless wire, and the load cell then generates a corresponding force signal. Fig.5 (b) shows the performance comparison of the calculated and the measured velocities. The estimated velocity using the Kalman filter is close to the calculated value from encoder. The estimated current appropriately follows the measured current as shown in Fig. 5 (c). Fig.4 (d) depicts the comparison results of the actual measured contact force from the load cell and the estimated force from the current output of the Kalman filter. The results confirm that the external force of the robot handle can be accurately estimated by the calculated current of the Kalman filter.

VI. Conclusion and Future Works

Approaches to control external contact forces of surgical manipulators have received increased attention in the development of MIS robot systems. To avoid the disadvantages of force sensor installation, an optional method that ensures the robustness and contact stability of a feedback control system is presented in this study. The external contact force was estimated by the driving current of the motor. A Kalman filter eliminates force noises and stable and reliable position responses can be achieved. The external force and device movements can be almost identically followed the tracks of the actual contact force and movements. Moreover, the proposed external force estimation approach can fuse the information of the optical encoder and current sensor.

The proposed external force estimation approach may be the key technology in future MIS robot systems. The proposed method can be applied to some other application areas, such as haptic device with reliable force feedback and robot-human cooperation systems with compliant motion.

References

[1] J.Rosen, B.Hannaford, M.P.MacFarlane, and M.N.Sinanan, "Force controlled and teleoperated endoscopic grasper for minimally invasive surgery-experimental performance evaluation," IEEE Trans. Biomed. Eng., vol.46, pp.1212-1221, 1999.

[2] A.L.Trejos, R.V.Patel, M.D.Naish, A.C.Lyle, and C.M.Schlachta, "A sensorized instrument for skills assessment and training in minimally invasive surgery," Journal of Medical Devices, vol.3, no.4, pp.041002-1-12, 2009.

[3] A.M.Okamura, L.N.Verner, T.Yamamoto, J.C.Gwilliam, and P.G.Griffiths, "Force feedback and sensory substitution for robot-assisted surgery," in Surgical Robotics. New York, NY, USA: Springer-Verlag, 2011, pp.419-448.

[4] M.B.Hong and Y.-H.Jo, "Design and evaluation of 2-dof compliant forceps with force-sensing capability for minimally invasive robot surgery," IEEE Trans. Robot., vol.28, no.4, pp.932-941, 2012.

[5] P.Baki, G.Szekely, and G. Kosa, "Design and characterization of a novel, robust, triaxial force sensor," Sensors Actuators A, Phys., vol.192, pp.101-110, 2013.

[6] Y.Hu, H.Jin, L.Zhang, P.Zhang, and J.Zhang, "State recognition of pedicle drilling with force sensing in a robotic spinal surgical system," IEEE/ASME Trans. Mechatron., vol.19, no.1, pp.357-365, 2014.

[7] D.-H.Lee, U.Kim, H.Moon, J.C.Koo, and H.R.Choi, "Development of multi-axial force sensing system for haptic feedback enabled minimally invasive robotic surgery," in Proc. IEEE/RSJ International Conference on Intelligent Robots and Systems, 2014, pp.4309-4314.

[8] U.Kim, D.-H.Lee, H.Moon, J.C.Koo, and H.R.Choi, "Design and realization of grasper-integrated force sensor for minimally invasive robotic surgery," in Proc. IEEE/RSJ International Conference on Intelligent Robots and Systems, 2014, pp.4321-4326.

[9] D.-H. Lee, U.Kim, T.Gulrez, W.J.Yoon, B.Hannaford, "A laparoscopic grasping tool with force sensing capability," IEEE/ASME Transactions on Mechatronics, vo.21, no.1, pp.130-141, 2016.

[10] U.Kim, D.-H.Lee, Y.B. Kim, D.-Y.Seok, J.So,and H.R.Choi, "S-Surge: Novel portable surgical robot with multi-axis force-sensing capability for minimally invasive surgery," IEEE/ASME Transactions on Mechatronics, Early view on line , pp.1-11, 2017.

[11] M.A.Qasaimeh, S.Sokhanvar, J.Dargahi, and M.Kahrizi, "PVDF based microfabricated tactile sensor for minimally invasive surgery," J. Microelectromech. Syst., vol.18, no.1, pp.195-207, 2009.

[12] J.Peirs, J.Clijnen, D.Reynaerts, H.van Brussel, P.Herijgers, B.Corteville,and S.Boone, "A micro optical force sensor for force feedback during minimally invasive robotic surgery," Sens. Actuators A, vol.115, pp.447-455, 2004.

[13] P.Puangmali, H.Liu, L.D.Seneviratne, P.Dasgupta, and K.Althoefer, "Miniature 3-axis distal force sensor for minimally invasive surgical palpation," IEEE/ASME Trans. Mechatron., vol.17, no.4, pp.646-656, 2012.

[14] R.Haslinger, R.Leyendecker, and U.Seibold, "A fiberoptic force-torque sensor for minimally invasive robotic surger," in Proc. IEEE Int. Conf. Robot. Autom., 2013, vol.2013, pp.4390-4395.

[15] T.Ohtsuka, A.Furuse, T.Kohno, J.Nakajima, K.Yagyu, and S.Omata,"Application of a new tactile sensor to thoracoscopic surgery: Experimental and clinical study," Ann. Thorac. Surg., vol.60, pp.610-614, 1995.

[16] E.Fetter, M.Biehl, and J.Meyer, "Vibrotactile palpation instrument for use in minimally invasive surgery," in Proc. IEEE Eng. Medicine Biol. Soc. Int. Conf., 1996, pp.179-180.

[17] I.Baumann, P.K.Plinkert, W.Kunert, and G.F.Buess, "Vibrotactile characteristics of different tissues in endoscopic otolaryngologic surgery-in vivo and ex vivo measurements," Min. Invas. Ther. Allied Technol., vol.10, no.6, pp.323-327, 2001.

[18] P.Puangmali,K. Althoefer, L.D.Seneviratne, "State-of-the-Art in force and tactile sensing for minimally invasive surgery," IEEE Sensors Journal, vol.8, no.4, pp.371-380, 2008.

[19] K.Ohishi, M.Miyazaki, and M.Fujita, "Hybrid control of force and position without force sensor," in Proc. IEEE International Conference on Industrial Electronics, San Diego, CA, USA,1992, pp. 670-675.

[20] H.Li, K.Kawashima, K. Tadano,S. Ganguly,S. Nakano, "Achieving haptic perception in forceps' manipulator using pneumatic artificial muscle," *IEEE/ASME Transactions on Mechatronics*, vol.18, no.1, pp.74 - 85, 2013.

[21] B.Zhao, and C.A.Nelson, "Tool-tissue force estimation for a 3-DOF robotic surgical tool," Proceedings of the ASME International Design Engineering Technical Conferences & Computers and Information in Engineering Conference, August 2-5, Boston, USA, 2015, pp.1-9.

[22] B.Zhao, and C.A.Nelson, "Sensorless force estimation for a three degrees-of-freedom motorized surgical grasper," Journal of Medical Devices, vol.9, no.3, pp. 030929-030929-3, 2015.

[23] B.Zhao, and C.A.Nelson, "Sensorless Force Sensing for Minimally Invasive Surgery," Journal of Medical Devices, vol.9, no.4, pp.041012-041012-14, 2015.

[24] Y.Li, M.Miyasaka, M.Haghighipanah, L.Cheng, and B.Hannaford, "Dynamic modeling of cable driven elongated surgical instruments forsensorless grip force estimation," in Proc. IEEE Int. Conf. Robot. Autom., 2016, pp.4128-4134.

[25] M.Haghighipanah, M.Miyasaka, and B.Hannaford, "Utilizing elasticity of cable driven surgical robot to estimate cable tension and external force," IEEE Robotics and Automation Letters, Preprint Version, pp.1-8, 2017.

[26] Y.Li,and B.Hannaford, "Gaussian process regression for sensorless grip force estimation of cable-driven elongated surgical instruments," IEEE Robotics and Automation Letters, vol.2, no.3, pp.1312-1320, 2017.

[27] H.Sang, J.Yun, R.Monfaredi, E.Wilson,H. Fooladi, K.Cleary, "External force estimation and implementation in robotically assisted minimally invasive surgery," The International Journal of Medical Robotics and Computer Assisted Surgery, Early View, pp.1-15, 2017.

[28] A.Kapoor, N.Simaan, P.Kazanzides, "A system for speed and torque control of DC motors with application to small snake robots," IEEE Conference on Mechatronics and Robotics, Aachen, Germany, 2004.

[29] G.S.Guthart and J.K.Salisbury, "The intuitive™ telesurgery system: Overview and application," in Proc. IEEE International Conference on Robotics and Automation, 2000, pp.618-621.